

Enhanced thermoelectric performance through crystal field engineering in transition metal–doped GeTe

Jing Shuai, Xiaojian Tan, Quansheng Guo, Jingtao Xu, A. Gellé, Régis Gautier, Jean-François Halet, Fainan Failamani, Jun Jiang, Takao Mori

▶ **To cite this version:**

Jing Shuai, Xiaojian Tan, Quansheng Guo, Jingtao Xu, A. Gellé, et al.. Enhanced thermoelectric performance through crystal field engineering in transition metal–doped GeTe. Materials Today Physics, 2019, 9, pp.100094. 10.1016/j.mtphys.2019.100094 . hal-02181617

HAL Id: hal-02181617

https://univ-rennes.hal.science/hal-02181617

Submitted on 10 Sep 2019

HAL is a multi-disciplinary open access archive for the deposit and dissemination of scientific research documents, whether they are published or not. The documents may come from teaching and research institutions in France or abroad, or from public or private research centers.

L'archive ouverte pluridisciplinaire **HAL**, est destinée au dépôt et à la diffusion de documents scientifiques de niveau recherche, publiés ou non, émanant des établissements d'enseignement et de recherche français ou étrangers, des laboratoires publics ou privés.

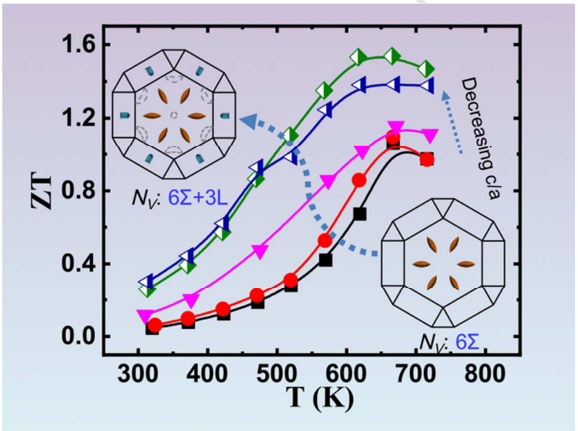
ACCEPTED MANUSCRIPT

Enhanced Thermoelectric Performance through Crystal Field Engineering in Transition Metal Doped GeTe

Jing Shuai,[1,⊥] *Xiaojian Tan,*[2,⊥] *Quansheng Guo,*[1] *Jingtao Xu,*[2] *Alain Gellé,*[3] *Régis Gautier,*[4] *Jean-François Halet,*[4] *Fainan Failamani,*[1] *Jun Jiang,*[2] *Takao Mori*[1,5,*]

[1] WPI International Center for Materials Nanoarchitechtonics (WPI-MANA) and Center for Functional Sensor & Actuator (CFSN), National Institute for Materials Science (NIMS), Namiki 1-1, Tsukuba 305-0044, Ibaraki, Japan
[2] Ningbo Institute of Materials Technology and Engineering, Chinese Academy of Sciences, Ningbo 315201, China
[3] Univ. Rennes, CNRS, Institut de Physique de Rennes – UMR 6251, F-35042 Rennes, France
[4] Univ. Rennes, Ecole Nationale Supérieure de Chimie de Rennes, CNRS, Institut des Sciences Chimiques de Rennes – UMR 6226, F-35042 Rennes, France
[5] Graduate School of Pure and Applied Sciences, University of Tsukuba, Tennoudai 1-1-1, Tsukuba 305-8671, Japan

TOC GRAPHICS



Highlights

- Enhanced Seebeck coefficient and decreased thermal conductivity upon Ti doping
- Further optimized thermoelectric performance by decreasing the carrier concentration and lattice thermal conductivity with co-doping Bi and Ti at Ge sites
- Proof of manipulating the crystal field effect as a feasible route of band engineering for the enhancement of the thermoelectric properties of the notable GeTe system

* Corresponding Authors. E-mail: mori.takao@nims.go.jp
⊥ These authors contributed equally.

Abstract

The change of multivalence band structure configuration between rhombodedral and cubic phase in GeTe offers additional dimension to modify its thermoelectric properties. Here, we report the synergetic optimization of electronic and thermal transport properties in rhombohedral GeTe doped with transition metal Ti. The Seebeck coefficient of $Ge_{1-x}Ti_xTe$ is significantly increased and the corresponding thermal conductivity is decreased. The structure refinement shows that Ti doping could reduce the lattice constant *c*/*a* ratio. Density functional theory calculations demonstrate that the affected crystal field rather than Ti orbitals is contributing to the valence band convergence and a Seebeck coefficient enhancement. Further optimization incorporates the effects of Bi substitution for reducing the carrier concentrations and introducing more point defects. This work not only confirms the transition metal elements as promising dopants for GeTe-based materials, but also indicates that the strategy of manipulating the crystal field effect can be exploited as a direct but effective route for improving thermoelectric performance.

The combination of economic, technological and environmental urgency has driven a growing prosperity in both the study of thermoelectricity and the exploration for new materials with superior thermoelectric properties in recent decades.[1-4] The critical issue that hinders its widespread utilization is the relatively low energy conversion efficiency, which is identified by the materials' thermoelectric dimensionless figure of merit $ZT = (S^2\sigma/\kappa)T$ (where S, σ, κ, and T are the Seebeck coefficient, electrical conductivity, thermal conductivity, and absolute temperature, respectively).[5] An ideal thermoelectric material must strike a balance between the conflicting requirements of high Seebeck coefficient S, high electrical conductivity σ, and low thermal conductivity κ (including both the electronic κ_e and phonon κ_l contributions).[6,7] The numerator $S^2\sigma$ is known as the power factor (*PF*). Previously effective strategies and concepts have been proposed to achieve higher *ZT*, such as modulation doping,[8,9] magnetic enhancement,[10-13] band engineering,[14-17] energy filtering effect,[18-21] *etc*. to improve the power factor, introducing nanostructure,[3,22-29] point defects,[30,31] *etc*. to compress the lattice thermal conductivity (κ_l), and exploring new materials with intrinsically low κ_l.[32-36]

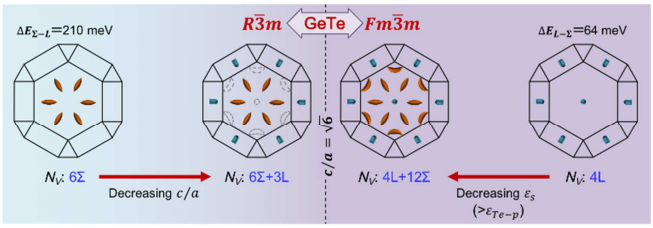
GeTe-based alloys, with their fascinating fundamental properties, have been known as promising thermoelectrics since 1960s but have not attracted as much attention as others IV-VI semiconductor analogs like PbTe-based materials.[37] The pristine GeTe undergoes a ferroelectric phase transition at the critical temperature around 700 K, in which the low-temperature rhombohedral structure ($R\bar{3}m$) changes to the high-temperature cubic structure ($Fm\bar{3}m$). Nowadays, the environmental concern regarding the restricted usage of Pb has brought the alternative GeTe alloys back into focus.[38,39] Most of the recent works have already suggested several routes for increasing the thermoelectric performance for GeTe systems, including the concept of structure influence as well as band structure modification and some designed lattice imperfections methods.[40-46]

Generally, doping of some elements or compounds will simultaneously affect the electronic and phonon transport behavior of thermoelectric materials. For thermal transport, it is commonly apparent that the naturally energy favorable Ge vacancies, large strain and mass fluctuation introduced by substitutional defects have enhanced phonon scattering, enabling a sufficiently reduced lattice thermal conductivity.[42,47,48] For electronic transport, the dopant orbitals may introduce perturbation to the band structure and electronic density of states, and also result in some structural change. For example, doping may modify the degree of the rhombohedral angle for more alignment of split bands, leading to the enhanced thermoelectric performance which happens in a rhombohedral phase but close to cubic.[40-42]

Previous works have discovered some suitable dopants to improve the thermoelectric properties of GeTe, such as $Ge_{1-x}Sb_xTe$,[49] $Ge_{1-x}Bi_xTe$,[40] $Ge_{1-x}Pb_xTe$,[43,50] $Ge_{1-x}In_xTe$,[51] $Ge_{1-x-y}Mn_xBi_yTe$,[44,52] $Ge_{1-x-y}Pb_xBi_yTe$,[41,53] $Ge_{1-x-y}Pb_xSb_yTe$,[42] $(GeTe)_{1-2x}(GeSe)_x(GeS)_x$,[54] $Ge_{1-x}P_xSb_yTe$,[55] $Ge_{1-x-y}In_xSb_yTe$,[46] $Ge_{1-x-y}Cd_xBi_yTe$,[45] $Ge_{1-x-y}Ga_xSb_yTe$,[56] *etc*. Besides, some doping elements are also reported to be detrimental to the final *ZT*, like Cu, Ag, Ba, Al, *etc*.[57],[58] One exception is that single Mn element substitution reduces the overall TE performance, while co-doping Mn with Sb or Bi suppresses the transition temperature and even realizes the higher *ZT* in cubic phase.[44,52] All of the aforementioned studies trigger our interests for searching for more potential doping elements, especially in the rarely studied transition metals groups. Moreover, the realized band engineering advancements are mainly "inertially" focusing on the cubic phase, mainly because GeTe shares many similarities with other cubic IV-VI semiconductors.[43-46] This aforesaid route also drives us to think more about a new concept to innovate the band engineering for the special GeTe-based system.

Scheme 1 illustrates the schematic diagram of valence band convergence for GeTe both for $R\bar{3}m$ and $Fm\bar{3}m$ phases. As it is known, the lattice of rhombohedral GeTe can be considered as a stretched cubic lattice along the body diagonal.[59] The lattice constant ratio *c*/*a* is 2.574 for rhombohedral GeTe while the equivalent value in cubic GeTe is 2.4495. For cubic GeTe, the character of valence bands is similar to those of other IV-VI compounds like PbTe or SnTe. The valence band maximum (VBM) of these cubic analogs is 4-

folded degenerate at the L point while the secondary one is 12-folded degenerate at theΣpoint of the Brillouin zone. A theoretical tight-binding model has demonstrated that the energy separation $\Delta E_{L\text{-}\Sigma}$ between L and Σ points could be reduced by dopants with *s* orbital energy higher than that of Te-*p* orbitals, such as Mg, Mn, Cd, *etc.*[60] $\Delta E_{L\text{-}\Sigma}$ of 64 meV for pristine cubic GeTe is small and the band convergence may be easy to realize, especially relative to SnTe. Indeed, the valence band convergence was achieved by Mn doping.[44] For rhombohedral GeTe, the valence band character is roughly similar to that of the cubic phase expect two differences. The valence band maximum is at the Σ point while the secondary ones are at the L point, and their degeneracies are decreased owing to the symmetry reduction of phase transition. The energy separation $\Delta E_{\Sigma\text{-}L}$ of pristine rhombohedral GeTe is about 210 meV. This work demonstrates that $\Delta E_{\Sigma\text{-}L}$ can be reduced by tuning the crystal field effect with the decreasing *c*/*a* ratio.



Scheme 1. Fermi surfaces illustrating the valence band convergence for rhombohedral (left) and cubic (right) GeTe. The crystal field effect (*c*/*a* ratio) and *s* orbital energy ($\varepsilon_s > \varepsilon_{Te\text{-}p}$) of dopant are the critical factor to realize band convergence in rhombohedral and cubic GeTe, respectively.

Herein, we investigate the thermoelectric properties of GeTe doped with Ti, which effectively tunes the crystal field effect to promote higher convergence of those multivalence band and then Seebeck coefficient. The total thermal conductivity is also dramatically decreased upon Ti doping, demonstrating Ti as one of the most effective transition metal doping elements for GeTe. In addition, co-doping Bi with Ti at Ge sites further optimizes thermoelectric performance by decreasing the carrier concentration and lattice thermal conductivity, leading to a superior thermoelectric figure of merit *ZT* of ~1.6 and making these alloys as top candidates for thermoelectric applications in middle temperature range.

Thermoelectric Properties of Ti-doped GeTe. The room temperature X-ray diffraction (XRD) patterns of $Ge_{1-x}Ti_xTe$ (x = 0, 0.01, 0.02, 0.03, 0.04 and 0.05) samples for low Ti concentration shown in Figure 1a closely match that of the rhombohedral phase GeTe. Doping with higher content of Ti gradually induces a partial phase transition. Rietveld refinements are carried out based on the powder X-ray diffraction data to estimate the lattice parameters. Detailed information is presented in Figure S1. With increasing content of Ti, the lattice parameter along the *c*-axis decreases from 10.669 Å for GeTe to 10.426 Å for $Ge_{0.995}Ti_{0.05}Te$, while the lattice *a* parameter gradually increases from 4.167 Å to 4.178 Å (Table 1). The overall effect is the decrease of the *c*/*a* ratio and also the unit cell volume, similar as the case in Mn-doped GeTe.[44]

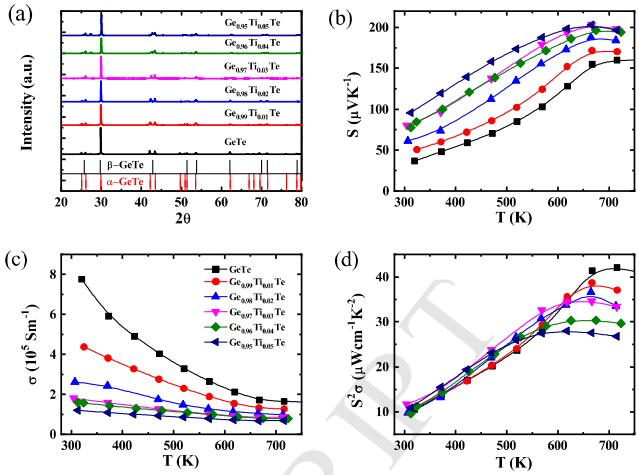


Figure 1. (a) XRD patterns of $Ge_{1-x}Ti_xTe$ (x = 0, 0.01, 0.02, 0.03, 0.04 and 0.05); temperature dependent electrical transport properties for all samples: (b) Seebeck coefficient, (c) electrical conductivity, and (d) power factor.

In Figure 1b, the measured Seebeck coefficient (*S*) shows an obvious increase upon Ti doping and saturates at higher temperatures when x reaches 0.05. Specifically, at 300 K *S* of 32 μV K^{-1} in the pristine GeTe increases to 94 μV K^{-1} in $Ge_{0.95}Ti_{0.05}Te$. The largely enhanced *S* demonstrates to be ascribed to the band convergence from changed crystal field effect upon Ti doping (see discussion later). Figure 1c shows the temperature-dependent electrical conductivity, which decreases with the raising of the content of Ti. However, the measured carrier concentrations of $Ge_{1-x}Ti_xTe$ compounds do not exhibit any obvious decreasing trend (Table 1). Thus, the significant decrease in electrical conductivity is mainly caused by the reduced carrier mobility. The opposite dependence relationship between carrier concentration and mobility observed here is supposed to be due to the increased density of ionized impurities when increasing the content of Ti doping. Compared with pristine GeTe, Ti doping decreases *PF* to some extent in the high temperature range (Figure 1d).

Table 1. Lattice Parameters (*a*, *c*), Room-temperature Carrier Concentrations (*n*) and Seebeck coefficients (*S*) of $Ge_{1-x}Ti_xTe$ (x = 0, 0.01, 0.02, 0.03, 0.04 and 0.05) Compositions

$Ge_{1-x}Ti_xTe$	*a* (Å)	*c* (Å)	*c*/*a*	*n* (10^{20} cm^{-3})	*S* (μV K^{-1})
x=0	4.1670	10.6695	2.5604	8.02	36.8
x=0.01	4.1671	10.6360	2.5524	7.19	50.8
x=0.02	4.1673	10.5875	2.5406	7.12	61.2
x=0.03	4.1693	10.5359	2.5270	6.18	80.3
x=0.04	4.1734	10.4807	2.5113	6.80	77.4
x=0.05	4.1781	10.4256	2.4953	8.04	95.5

Band Convergence Caused by Changed Crystal Field Effect. To better understand the improved Seebeck coefficient of the Ti-doped GeTe compounds, density functional theory (DFT) calculations were carried out to examine the density of states (DOS) and band structure. Firstly, we constructed a supercell including Ti atom to calculate the possible distortion

of the DOS for $Ge_{1-x}Ti_xTe$, and present the results in Figure S2 in the Supporting Information. Considering that the transition element possesses contracted 3*d* orbitals, it should be careful to determine the ground state of transition element-doped system. Taking Mn doping as an example, Mn^{2+} ion has 5 *d*-electrons in Mn-doped IV-VI compounds. In the nonmagnetic state, Mn doping always introduces some flat bands around the Fermi level and leads to a strong Stoner instability. In the ferromagnetic ground state, the spin-up *d*-bands are fully occupied and the spin-down *d*-bands are fully empty. Owing to this magnetic exchange splitting, the Mn-*d* orbitals are pushed away from the Fermi level and Mn-doping will not show *d*-resonant levels. For the doped elements which have less (Sc, Ti, Cr) or more *d*-electrons (Fe, Co, Ni) than Mn, there will certainly be resonant levels near the Fermi level because of the existence of partly spin-up or spin-down channels, respectively.[44,61] Since the energy of Ti *d* orbitals (–11.05 eV) is higher than that of Mn *d* ones (–15.27 eV),[62] the resonant level of the Ti-doped system will be close to the bottom of the conduction band. As it may be seen in Figure S2, Ti doping introduces resonant DOS at the upper edge of the band gap and has less effect on the valence band, which is consistent with the above theoretical analysis.

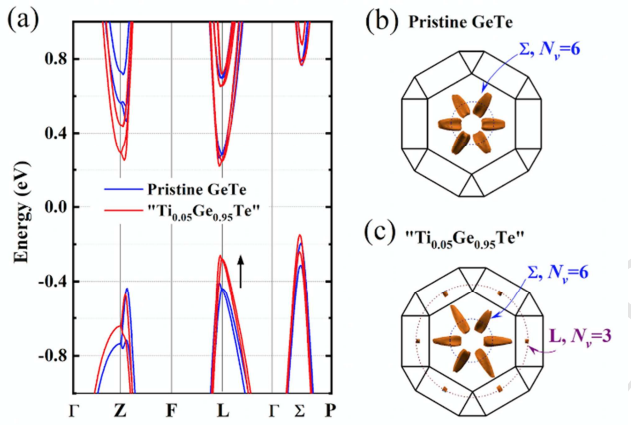


Figure 2. (a) Calculated band structure of pristine GeTe and equivalent "$Ge_{0.95}Ti_{0.05}Te$". (b) and (c) are the corresponding Fermi surfaces when the hole concentration is 5 × 10^{20} cm^{-3}.

Now that the electronic orbitals of Ti are not likely the reason of enhanced Seebeck coefficient of *p*-type $Ge_{1-x}Ti_xTe$, we thus focus on the changed lattice constant and the corresponding crystal field effect by Ti doping. As the Ti content *x* increasing, the values of *c*/*a* become smaller and smaller, which is also equivalent to the degree of rhombohedral angle approaching 90 degrees. To elucidate the influence of crystal field effect variation on the VBMs, the band structures of pristine and "Ti-doped" GeTe are calculated and shown in Figure 2a. Here, we model the Ti-doped GeTe by a primitive GeTe cell with changed lattice constants *a* and *c* according to the experimental results given in Table 1. This method has been adopted in the previous report about rhombohedral IV-VI GeSe compound.[63] As it may be seen, the secondary VBM at the L point moves up to be close to the first VBM at the Σ point, and the energy separation $\Delta E_{\Sigma\text{-}L}$ is decreased from 210 meV of pristine GeTe to 110 meV of "$Ge_{0.95}Ti_{0.05}Te$". In order to better visualize the band valley variation, the Fermi surfaces at the hole concentration of 5 × 10^{20} cm^{-3} for pristine GeTe and "$Ge_{0.95}Ti_{0.05}Te$" are shown in Figure 2b and 2c, respectively. It is interesting to find that the valley number N_V increases from 6 to 9 in Ti-doped GeTe. Such an increased N_V is very beneficial to improve the DOS effective mass and Seebeck coefficient.

The detailed temperature dependent electronic thermal conductivity κ_e, lattice thermal conductivity κ_l, as well as Lorenz factor *L* for $Ge_{1-x}Ti_xTe$ alloys are shown in Figure S3. The decline in κ_e originates from the increased electrical resistivity upon Ti doping and the decrease in κ_l is largely due to the mass and size fluctuation with Ti substitution. Figure S3d shows *ZT* as a function of temperature, in which a maximum *ZT* ~1.2 is implemented in $Ge_{0.98}Ti_{0.02}Te$, higher than most reported transition metal doping elements.[44,45,57]

Thermoelectric Properties of Ti-Bi Co-doped GeTe. Even though Ti-doped GeTe compounds exhibit significantly enhanced Seebeck coefficients, the carrier concentrations and lattice thermal conductivity are still far from the ideal range in which the optimized thermoelectric performance could be possibly achieved.[40,42,44] For further improving the TE properties in GeTe thermoelectrics, we took into account the effects of Ti doping with $Ge_{0.99}Ti_{0.01}Te$, which shows relatively better electrical transport properties, and continuously substituted Bi in Ge site to form $Ge_{0.99-y}Ti_{0.01}Bi_yTe$ (y = 0.04, 0.05, 0.06, 0.07) compositions (for comparison, the properties of the optimized Bi-doped GeTe are given in the supporting information, Figure S4).

The room-temperature powder XRD patterns for the synthesized $Ge_{0.99-y}Ti_{0.01}Bi_yTe$ compounds are shown in Figure S5. Doping with Bi is found to be effective for decreasing the lattice *c*-axis parameter, while increasing the lattice *a*-axis parameter (Table 2), contributing overall in reducing the *c*/*a* ratio as observed for Ti doping. The successful Bi substitution with Ti in Ge site also effectively reduces the carrier concentration as low as to ~2 × 10^{20} cm^{-3}.

To shed light on the influence of the modified band structure on the charge transport for both Ti-doped and Ti-Bi co-doped cases, we compare the room temperature plots of *S* versus the carrier concentration *n* in Figure 3a. Obviously, alloying and doping nicely enable a broad range of carrier concentration to be achieved, which ensures a further optimal carrier concentration to be located for maximizing the electronic performance in Ti/Bi co-doping samples. Here, compared with the valence +2 of Ge, Bi serves as the electron donor with the valence of +3, whereas Ti doping has negligible effect for modifying the carrier concentration with the formal valence of +2. Importantly, the doping effect of both Ti and Bi leads to the significant enhancement of DOS effective mass m^*, which is demonstrated by the calculated Pisarenko relation displayed as black dashed lines in Figure 3a. Therefore, both enlarged m^* due to the band structure modified by Ti/Bi and decreased carrier concentration to the optimal level by Bi are achieved at the same time.

Table 2. Lattice Parameters, Room-temperature Carrier Concentrations and Seebeck Coefficients of $Ge_{0.99-y}Ti_{0.01}Bi_yTe$ Compositions.

$Ge_{0.99-y}Ti_{0.01}Bi_yTe$	*a* (Å)	*c* (Å)	*c*/*a*	*n* (10^{20} cm^{-3})	*S* (μV K^{-1})

y=0.04	4.1862	10.6091	2.5343	3.37	82.6
y=0.05	4.1912	10.5939	2.5277	3.23	94.9
y=0.06	4.1961	10.5785	2.5210	2.59	109.0
y=0.07	4.2006	10.5572	2.5132	2.29	130.3

As a consequence, *S* increases and electrical conductivity decreases with increasing Bi-doping in the entire temperature, shown in Figure 3b and 3c. Particularly, two peaks appear in the temperature-dependent *S* trend with x = 0.07. The first peak is ascribed to the valence band switch in energy at the L and Σ points, which is a common phenomenon associated with the phase transition. The second peak is mainly due to the bipolar effect. Although the peak of the power factor does not increase upon co-doping, the low temperature power factors have been improved for all the co-doped samples, as shown in Figure 3d. And the average power factors of $Ge_{0.99-y}Ti_{0.01}Bi_yTe$ (x = 0.04, 0.05, 0.06) are also higher than that of the pristine GeTe (Figure S6).

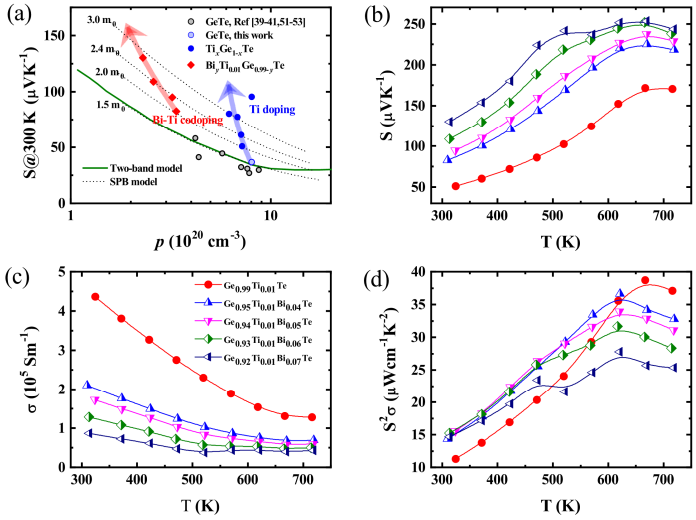


Figure 3. (a) Room temperature carrier concentration dependent Seebeck coefficient for Ti doping and Ti/Bi co-doping samples; temperature dependent electrical transport properties for all samples, (b) Seebeck coefficient, (c) electrical conductivity, and (d) power factor.

Because of both reduced electrical thermal conductivity κ_e due to the increased carrier concentration and further reduced lattice thermal conductivity κ_l caused by the substitution of strengthening the phonon scattering, the total thermal conductivity considerably decreases over the entire temperature range with increasing Bi concentration. The calculated κ_e values according to the Wiedemann-Franz law and Lorenz factor are summarized in Figure S7. It is well known that the Ge vacancies have a non-negligible effect, which contribute to lowering the lattice thermal conductivity. To quantitatively understand the influence of these cationic vacancies and the point defects by Ti/Bi substitution on the lattice thermal conductivity, we numerically investigated the phonon transport properties using the Debye-Callaway model by taking into account phonon-phonon and point-defects scattering mechanisms. Room-temperature reduction in κ_l can be well understood by this model, which clearly indicates that stronger effect on the reduction of the lattice thermal conductivity is obtained by Ti/Bi substitution (Figure 4c).

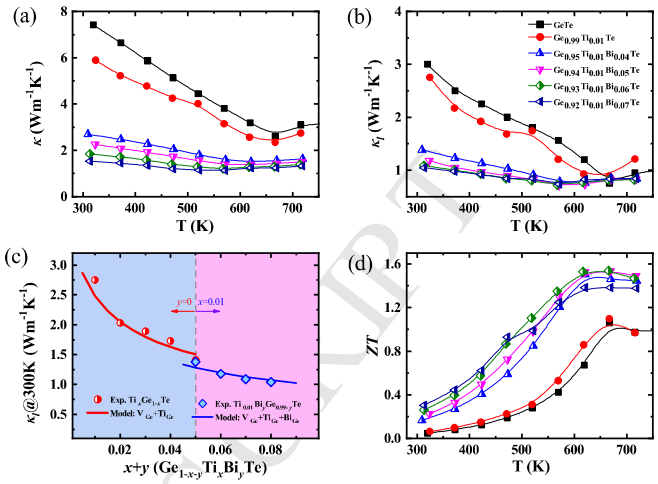


Figure 4. Temperature dependent thermoelectric transport properties for Ti doping and Ti/Bi co-doping samples $Ge_{0.99-y}Ti_{0.01}Bi_yTe$ (y = 0, 0.04, 0.05, 0.06, 0.07): (a) total thermal conductivity, (b) lattice thermal conductivity, (c) Composition dependent lattice thermal conductivity for all samples at room temperature, with a comparison to Debye-Callaway model predictions, (d) figure of merit *ZT*.

The effects of band convergence due to Ti doping, optimization of carrier concentration, and a simultaneously enhanced phonon scattering by additional Bi doping finally contribute to the further enhancement in the thermoelectric figure of merit *ZT*, as shown in Figure 4d. The highest *ZT* of 1.6 is achieved for $Ge_{0.93}Ti_{0.01}Bi_{0.06}Te$ at 623 K, much higher than that of pristine GeTe and also comparable with those of previous reports.[44,52] Therefore, we have demonstrated the high thermoelectric performance of bulk GeTe-based materials through the strategy of manipulating crystal field effect and point defects effect, making these doped materials as top candidates for thermoelectric applications in middle temperature range.

In summary, it has been experimentally demonstrated that Ti is one of the most effective transition metal dopants for enhancing the thermoelectric performance of pristine GeTe. This is due to the dual effect of both increased Seebeck coefficient and the corresponding decreased thermal conductivity of $Ge_{1-x}Ti_xTe$. Further optimization incorporates the effects of Bi substitution for reducing the carrier concentrations and introducing more point defects, as indicated by the simulation study of phonon transport using the Debye-Callaway model. First-principles density functional theory calculations show that the energy separation $\Delta E_{\Sigma\text{-}L}$ can be reduced by tuning the crystal field effect with the decreasing of c/a ratio. Moreover, the valley number even increases upon Ti doping, which is beneficial to improve the DOS effective mass and Seebeck coefficient. With the high *ZT* value of 1.6 achieved for $Ge_{0.93}Ti_{0.01}Bi_{0.06}Te$ at 623 K, this study has proved nicely that manipulating the crystal field effect is a feasible route of band engineering for the enhancement of the thermoelectric properties of the notable GeTe system.

Acknowledgment

This work was supported by the International Research Fellow of Japan Society for the Promotion of Science (Postdoctoral Fellowships for Research in Japan (Standard)). X.T. was supported by the National Natural Science Foundation of China (21875273), Youth Innovation Promotion Association of Chinese Academy of Sciences (2019337), and Ningbo Municipal Natural Science Foundation (2018A610077). Support from CREST JPMJCR15Q6 and JSPS KAKENHI JP17H02749, JP16H06441, JP18F18374 is also acknowledged. These studies were also facilitated within the scope of the France Japan International Collaboration Framework through the Laboratory for Innovative Key Materials and Structures (UMI 3629 LINK), financially supported by Saint-Gobain, Centre National de la Recherche Scientifique (CNRS), Université de Rennes 1 (UR1), and National Institute for Materials Science (NIMS).

Supporting Information

Brief statement of detailed method for samples synthesis, physical characterization, density functional theory calculations, and Debye-Callaway model. Rietveld refinement, calculated density of state, and temperature dependent transport coefficients for Ti-doped and Ti-Bi codoped GeTe samples are also included.

Notes

The authors declare no competing financial interest.

References

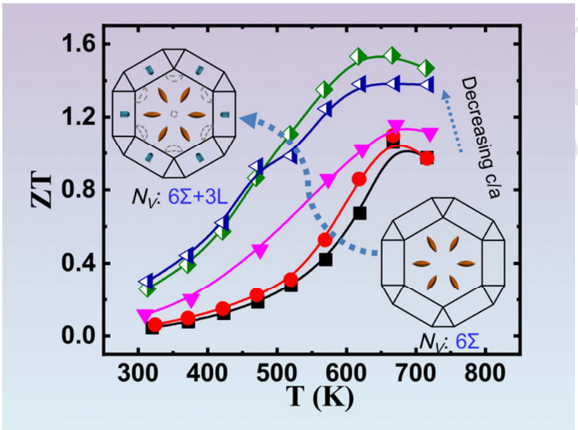
[1] F. J. DiSalvo, *Science* **1999**, *285*, 703.
[2] M. S. Dresselhaus, G. Chen, M. Y. Tang, R. G. Yang, H. Lee, D. Z. Wang, Z. F. Ren, J. P. Fleurial, P. Gogna, *Adv. Mater.* **2007**, *19*, 1043.
[3] W. Liu, J. Hu, S. Zhang, M. Deng, C. Han, Y. Liu, *Materials Today Physics* **2017**, *1*, 50.
[4] I. Petsagkourakis, K. Tybrandt, X. Crispin, I. Ohkubo, N. Satoh, T. Mori, *Sci. Tech. Adv. Mater.* **2018**, *19*, 836.
[5] G. J. Snyder, E. S. Toberer, *Nat Mater* **2008**, *7*, 105.
[6] T. Mori, *Small* **2017**, *13*, 1702013.
[7] J. Mao, Z. Liu, J. Zhou, H. Zhu, Q. Zhang, G. Chen, Z. Ren, *Advances in Physics* **2018**, *67*, 69.
[8] M. Zebarjadi, G. Joshi, G. Zhu, B. Yu, A. Minnich, Y. Lan, X. Wang, M. Dresselhaus, Z. Ren, G. Chen, *Nano Lett.* **2011**, *11*, 2225.
[9] B. Yu, M. Zebarjadi, H. Wang, K. Lukas, H. Wang, D. Wang, C. Opeil, M. Dresselhaus, G. Chen, Z. Ren, *Nano Lett.* **2012**, *12*, 2077.
[10] R. Ang, A. U. Khan, N. Tsujii, K. Takai, R. Nakamura, T. Mori, *Angew. Chem.* **2015**, *127*, 13101.
[11] F. Ahmed, N. Tsujii, T. Mori, *J. Mater. Chem. A*, **2017**, *5*, 7545.
[12] H. Takaki, K. Kobayashi, M. Shimono, N. Kobayashi, K. Hirose, N. Tsujii, T. Mori, *Materials Today Physics* **2017**, *3*, 85.
[13] N. Tsujii, A. Nishide, J. Hayakawa, T. Mori, *Sci. Adv.* **2019**, *5*, eaat5935.
[14] W. Liu, X. Tan, K. Yin, H. Liu, X. Tang, J. Shi, Q. Zhang, C. Uher, *Phys. Rev. Lett.* **2012**, *108*, 166601.
[15] Q. Zhang, F. Cao, W. Liu, K. Lukas, B. Yu, S. Chen, C. Opeil, D. Broido, G. Chen, Z. Ren, *J. Am. Chem. Soc.* **2012**, *134*, 10031.
[16] Y. Pei, H. Wang, G. J. Snyder, *Adv. Mater.* **2012**, *24*, 6125.
[17] C. Fu, T. Zhu, Y. Liu, H. Xie, X. Zhao, *Energy Environ. Sci.* **2014**, *8*, 216.
[18] D. Vashaee, A. Shakouri, *Phys. Rev. Lett.* **2004**, *92*, 106103.
[19] J. P. Heremans, C. M. Thrush, D. T. Morelli, *Phys. Rev. B* **2004**, *70*, 115334.
[20] J. Martin, L. Wang, L. Chen, G. S. Nolas, *Phys. Rev. B* **2009**, *79*, 115311.
[21] A. Pakdel, Q. Guo, V. Nicolosi, T. Mori, *J. Mater. Chem. A* **2018**, *6*, 21341.
[22] K. F. Hsu, S. Loo, F. Guo, W. Chen, J. S. Dyck, C. Uher, T. Hogan, E. K. Polychroniadis, M. G. Kanatzidis, *Science* **2004**, *303*, 818.
[23] M. Zhou, J.-F. Li, T. Kita, *J. Am. Chem. Soc.* **2008**, *130*, 4527.
[24] B. Poudel, Q. Hao, Y. Ma, Y. Lan, A. Minnich, B. Yu, X. Yan, D. Wang, A. Muto, D. Vashaee, X. Chen, J. Liu, M. S. Dresselhaus, G. Chen, Z. Ren, *Science* **2008**, *320*, 634.
[25] G. Joshi, H. Lee, Y. Lan, X. Wang, G. Zhu, D. Wang, R. W. Gould, D. C. Cuff, M. Y. Tang, M. S. Dresselhaus, G. Chen, Z. Ren, *Nano Lett.* **2008**, *8*, 4670.
[26] J. R. Sootsman, D.-Y. Chung, M. G. Kanatzidis, *Angew. Chem.* **2009**, *48*, 8616.
[27] Y. Lan, A. J. Minnich, G. Chen, Z. Ren, *Adv. Funct. Mater.* **2010**, *20*, 357.
[28] J.-F. Li, W.-S. Liu, L.-D. Zhao, M. Zhou, *NPG Asia Mater* **2010**, *2*, 152.
[29] A. U. Khan, K. Kobayashi, D. Tang, Y. Yamauchi, K. Hasegawa, M. Mitome, Y. Xue, B. Jiang, K. Tsuchiya, D. Golberg, Y. Bando, T. Mori, *Nano Energy* **2017**, 31, 152-159.
[30] J. Yang, G. P. Meisner, L. Chen, *Appl. Phys. Lett.* **2004**, *85*, 1140.
[31] C. Hu, K. Xia, X. Chen, X. Zhao, T. Zhu, *Materials Today Physics* **2018**, *7*, 69.
[32] L.-D. Zhao, S.-H. Lo, Y. Zhang, H. Sun, G. Tan, C. Uher, C. Wolverton, V. P. Dravid, M. G. Kanatzidis, *Nature* **2014**, *508*, 373.
[33] K. Zhao, P. Qiu, Q. Song, A. Blichfeld, E. Eikeland, D. Ren, B. Ge, B. Iversen, X. Shi, L. Chen, *Materials Today Physics* **2017**, *1*, 14.
[34] S. Lin, W. Li, Z. Bu, B. Gao, J. Li, Y. Pei, *Materials Today Physics* **2018**, *6*, 60.
[35] J. Shuai, J. Mao, S. Song, Q. Zhang, G. Chen, Z. Ren, *Materials Today Physics*, **2017**, *1*, 75.
[36] C. Chang, L.-D. Zhao, *Materials Today Physics* **2018**, *4*, 50.
[37] F. D. Rosi, J. P. Dismukes, E. F. Hockings, *Electrical Engineering* **1960**, *79*, 450.
[38] S. Perumal, S. Roychowdhury, K. Biswas, *J. Mater. Chem. C* **2016**, *4*, 7520.
[39] S. Roychowdhury, M. Samanta, S. Perumal, K. Biswas, *Chem. Mater.* **2018**, *30*, 5799.
[40] J. Li, Z. Chen, X. Zhang, Y. Sun, J. Yang, Y. Pei, *NPG Asia Mater* **2017**, *9*, e353.
[41] J. Li, X. Zhang, Z. Chen, S. Lin, W. Li, J. Shen, I. T. Witting, A. Faghaninia, Y. Chen, A. Jain, L. Chen, G. J. Snyder, Y. Pei, *Joule* **2018**, *2*, P976.
[42] J. Li, X. Zhang, X. Wang, Z. Bu, L. Zheng, B. Zhou, F. Xiong, Y. Chen, Y. Pei, *J. Am. Chem. Soc.* **2018**, *140*, 16190.
[43] Y. Gelbstein, J. Davidow, S. N. Girard, D.-Y. Chung, M. Kanatzidis, *Adv. Energy Mater.* **2013**, *3*, 815.
[44] Z. Zheng, X. Su, R. Deng, C. Stoumpos, H. Xie, W. Liu, Y. Yan, S. Hao, C. Uher, C. Wolverton, M. G. Kanatzidis, X. Tang, *J. Am. Chem. Soc.* **2018**, *140*, 2673.
[45] M. Hong, Y. Wang, W. Liu, S. Matsumura, H. Wang, J. Zou, Z.-G. Chen, *Adv. Energy Mater.* **2018**, *8*, 1801837.
[46] M. Hong, Z.-G. Chen, L. Yang, Y.-C. Zou, M. S. Dargusch, H. Wang, J. Zou, *Adv. Mater.* **2018**, *30*, 1705942.
[47] F. Serrano-Sánchez, M. Funes, N. M. Nemes, O. J. Dura, J. L. Martínez, J. Prado-Gonjal, M. T. Fernández-Díaz, J. A. Alonso, *Appl. Phys. Lett.* **2018**, *113*, 083902.
[48] X. Zhang, J. Li, X. Wang, Z. Chen, J. Mao, Y. Chen, Y. Pei, *J. Am. Chem. Soc.* **2018**, *140*, 15883.
[49] S. Perumal, S. Roychowdhury, D. S. Negi, R. Datta, K. Biswas, *Chem. Mater.* **2015**, *27*, 7171.
[50] J. Li, Z. Chen, X. Zhang, H. Yu, Z. Wu, H. Xie, Y. Chen, Y. Pei, *Adv. Sci.* **2017**, *4*, 1700341.

[51] L. Wu, X. Li, S. Wang, T. Zhang, J. Yang, W. Zhang, L. Chen, J. Yang, *NPG Asia Mater* **2017**, *9*, e343.
[52] Z. Liu, J. Sun, J. Mao, H. Zhu, W. Ren, J. Zhou, Z. Wang, D. J. Singh, J. Sui, C.-W. Chu, Z. Ren, *Proc Natl Acad Sci USA* **2018**, *115*, 5332.
[53] D. Wu, L.-D. Zhao, S. Hao, Q. Jiang, F. Zheng, J. W. Doak, H. Wu, H. Chi, Y. Gelbstein, C. Uher, C. Wolverton, M. Kanatzidis, J. He, *J. Am. Chem. Soc.* **2014**, *136*, 11412.
[54] M. Samanta, K. Biswas, *J. Am. Chem. Soc.* **2017**, *139*, 9382.
[55] J. Rajeev Gandhi, R. Nehru, S.-M. Chen, R. Sankar, K. S. Bayikadi, P. Sureshkumar, K.-H. Chen, L.-C. Chen, *CrystEngComm* **2018**, *20*, 6449.
[56] B. Srinivasan, A. Gellé, F. Gucci, C. Boussard-Pledel, B. Fontaine, R. Gautier, J.-F. Halet, M. J. Reece, B. Bureau, *Inorg. Chem. Front.* **2019**, *6*, 63.
[57] B. Srinivasan, R. Gautier, F. Gucci, B. Fontaine, J.-F. Halet, F. Cheviré, C. Boussard-Pledel, M. J. Reece, B. Bureau, *J. Phys. Chem. C* **2017**, *122*, 227.
[58] B. Srinivasan, A. Gellé, J.-F. Halet, C. Boussard-Pledel, B. Bureau, *Materials* **2018**, *11*, 2237.
[59] T. Chattopadhyay, J. X. Boucherle, H. G. vonSchnering, *J. Phys. C: Solid State Phys.* **2000**, *20*, 1431.
[60] X. Tan, H. Wang, G. Liu, J. G. Noudem, H. Hu, J. Xu, H. Shao, J. Jiang, *Materials Today Physics* **2018**, *7*, 35.
[61] X. Tan, H. Shao, T. Hu, G.-Q. Liu, S.-F. Ren, *J. Phys.: Condens. Matter* **2015**, *27*, 095501.
[62] W. A. Harrison, *Elementary Electronic Structure*, *World Scientific, Singapore* **2003**.
[63] M. Yan, X. Tan, Z. Huang, G. Liu, P. Jiang, X. Bao, *J. Mater. Chem. A* **2018**, *6*, 8215.

ACCEPTED MANUSCRIPT

Highlights

- Enhanced Seebeck coefficient and decreased thermal conductivity upon Ti doping
- Further optimized thermoelectric performance by decreasing the carrier concentration and lattice thermal conductivity with co-doping Bi and Ti at Ge sites
- Proof of manipulating the crystal field effect as a feasible route of band engineering for the enhancement of the thermoelectric properties of the notable GeTe system



ACCEPTED MANUSCRIPT